MODEL BASED INERTIAL SENSING OF HUMAN BODY MOTION KINEMATICS IN SIT-TO-STAND MOVEMENT

Josip Musić[1], Roman Kamnik[2], Marko Munih[2]

[1]University of Split, Faculty of Electrical Engineering, Mechanical Engineering and Naval Architecture
21000 Split, Ruđera Boškovića bb, Croatia
[2]University of Ljubljana, Faculty of Electrical Engineering
1000 Ljubljana, Tržaška 25, Slovenia

jmusic@fesb.hr (Josip Musić)

Abstract

In this paper the design and validation of three-segment human body model is presented. The model is aimed at reconstruction of motion trajectories of shank, thigh and HAT (Head-Arms-Trunk) segments in sit-to-stand transfer. For this purpose the Extended Kalman filter (EKF) is applied for fusion of model data and data acquired through measurements with low cost inertial motion sensors (consisting of accelerometers and rate gyroscopes). The simplifications, like motion constraint to sagittal plane, symmetry of movement, assumption of ideal joints, etc., are introduced in the model. Three-segment human body model is constructed using principles of Lagrangian dynamics resulting in three nonlinear, highly coupled second order differential equations. From these equations human body model in Matlab- Simulink environment is constructed and implemented. In conjunction with classical definition of angle, angular rate of change and angular acceleration one can get complete set of data describing human sit-to-stand movement. The inputs that were used in the modeling phase include moments at three joints (ankle, knee and hip joint) by using inverse dynamic approach and free-body diagram technique. Calculated moments include both active and passive joint moments. Several EKF architectures were tested in search for optimal performance. Model validation (in conjunction with EKF) was performed on simulated data using Matlab-Simulink environment, and on actual measurements data acquired with Optotrak optical motion analysis system. Obtained results are presented and discussed, and conclusions are drawn.

Keywords: lagrangian dynamics, sit-to-stand, extended kalman filter

Presenting Author's biography

Josip Musić. Received the Electrical Engineering diploma in 2004 from the Faculty of Electrical Engineering and Naval Architecture, University of Split, Croatia, where he is currently employed as a research/teaching assistant. He is currently a postgraduate student at Faculty of Electrical Engineering, University of Ljubljana, Slovenia. His current research interests include human motion analysis and inertial sensing.

1 Background

Over the last few years the miniature inertial sensors have become widely available. Because of their low cost and miniature size they are practical for wide range of applications such as biomechanical analysis of human motion [1,2,3,4,5,6], virtually reality [7], ergonomic studies [8] etc.

In dynamic analysis of rigid body motion, the knowledge of translational and angular velocities and accelerations of body center of mass is crucial [5,9]. Traditionally these variables are measured by optical motion tracking systems (like Optotrak-Northern Digital Inc.). However, these systems have number of shortcomings, as are: high cost, restriction to laboratory settings, markers are easily obscured, markers require time-consuming setting up procedure etc. More recently, body mounted inertial sensors have been used for measurement of kinematic data [3,4,5,7]. These sensors consist of accelerometers and gyroscopes mounted in the casing which is then attached to measured human body segment whose kinematic parameters are of interest.

Inertial sensors (accelerometers and gyroscopes) are not without errors [5]: two accelerometer signal components, the dynamic and gravitational, can't easily be distinguished during faster movements while drift of the gyroscope output results in large integration errors. The accuracy can be improved by adding magnetometer to the inertial sensor setup, and using Kalman filtering techniques for data fusion with accelerometer and gyroscope data [6,7]. This technique is widely used and shows good results under certain restrictions, one of them is lack of large metal or magnetic objects in the vicinity [10]. Such objects can potentially introduce disturbance signal to the magnetometer readings.

In this study we assume that magnetometers can (in certain applications) be substituted by incorporation of dynamic human body model [4,11]. In this approach the Extended Kalman Filtering (EKF) technique is used to fuse data acquired from inertial sensor measurements (accelerometers and gyroscopes) with data from the dynamic human model. In this way we believe that better kinematic measurements in ambulatory settings where number of metallic objects and instruments (with their electromagnetic fields) exist are possible.

Paper presents the development and validation of proposed method for model based inertial sensing of human body motion kinematics in sit-to-stand movement. The structure of this paper is as follows. In Section 2 three-segment dynamic human body model is constructed and described. Then Extended Kalman Filter is designed to incorporate all necessary measurements and estimates. In Section 3 results for simulated and measured data are presented and discussed. Finally in Section 4 some conclusions are drawn based on acquired results.

2 Materials and methods

2.1 Model description

The proposed three-segment human body model in sit-to-stand transition [11] is restricted in the two-dimensional (sagittal) plane and consists of three segments: shank, thigh and HAT (Head-Arms Trunk). Restriction to the sagittal plane is valid if symmetry of sit-to-stand movement is assumed. The segments are represented as rigid bodies with their masses contained at center of mass (Figure 1). Joints are assumed to be ideal with no added friction during rotation. Inputs to the model are joint moments M_1, M_2 and M_3 at ankle, knee and hip joint respectively. These moments are calculated using Newton-Euler inverse dynamic approach [2,9] based on data measured by optical motion tracking system and force plate(s).

Mathematical description of three-segment sit-to-stand model is based on Lagrangian dynamics approach. In that approach well known equations of motion for rigid body are derived from

$$\frac{d}{dt}\left(\frac{\partial L}{\partial \dot{\Theta}_i}\right) - \frac{\partial L}{\partial \Theta_i} = T_i \qquad i=1,2,3 \qquad (1)$$

where: L – Lagrangian function (L=K-V)

T – generalized forces/moments on i-th segment

K – kinetic energy of *i*-th segment

V – potential energy of *i*-th segment

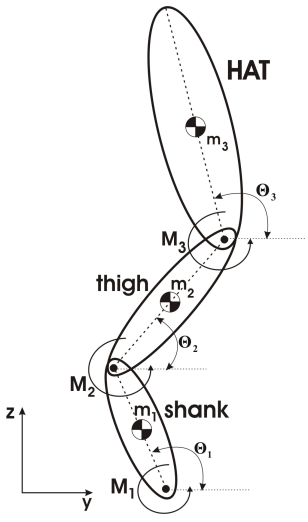

Fig. 1 Three segment human body model

Using Lagrangian dynamics and model notation in Figure 1 the following equations are derived:

$$\ddot{\Theta}_1(m_1c_1^2+m_2l_1^2+m_3l_1^2+I_{x1})+\ddot{\Theta}_2\cos(\Theta_1-\Theta_2)(m_2l_1c_2+m_3l_1l_2)+\ddot{\Theta}_3\cos(\Theta_1-\Theta_3)m_3l_1c_3+$$
$$\dot{\Theta}_2^2\sin(\Theta_1-\Theta_2)(m_2l_1c_2+m_3l_1l_2)+\dot{\Theta}_3^2\sin(\Theta_1-\Theta_3)m_3l_1c_3+g(m_1c_1+m_2l_1+m_3l_1)\cos\Theta_1=M_1-M_2 \quad (2)$$

$$\ddot{\Theta}_2(m_2c_2^2+m_3l_2^2+I_{x2})+\ddot{\Theta}_1\cos(\Theta_1-\Theta_2)(m_2l_1c_2+m_3l_1l_2)+\ddot{\Theta}_3\cos(\Theta_2-\Theta_3)m_3l_2c_3-$$
$$\dot{\Theta}_1^2\sin(\Theta_1-\Theta_2)(m_2l_1c_2+m_3l_1l_2)+\dot{\Theta}_3^2\sin(\Theta_2-\Theta_3)m_3l_2c_3+g(m_2c_2+m_3l_2)\cos\Theta_2=M_2-M_3 \quad (3)$$

$$\ddot{\Theta}_3(m_3c_3^2+I_{x3})+\ddot{\Theta}_1\cos(\Theta_1-\Theta_3)m_3l_1c_3+\ddot{\Theta}_2\cos(\Theta_2-\Theta_3)m_3l_2c_3-$$
$$\dot{\Theta}_1^2\sin(\Theta_1-\Theta_3)m_3l_1c_3-\dot{\Theta}_2^2\sin(\Theta_2-\Theta_3)m_3l_2c_3+gm_3c_3\cos\Theta_3=M_3 \quad (4)$$

where

l_i - segment length,

c_i - distance of segmental CoM from distal joint,

I_{xi} - segmental moment of inertia.

Equations (2), (3) and (4) describe the motion of the shank, thigh and HAT segment, respectively. Segmental masses, lengths, center-of-mass (CoM) positions and moments of inertia are calculated using anthropometric data [12].

As it can be seen, the above equations form non-linear, highly coupled system of differential equations. Outputs from the model are angle, angular rate and angular acceleration for every segment from which linear acceleration can be calculated.

2.2 Extended Kalman Filter design

In the proposed approach the Extended Kalman filter has a key role. It is aimed for fusion of data acquired through measurements with data obtained from developed dynamic human body model. Kalman filtering is a common approach in multisignal integration tasks [7,9]. In EKF, the model is represented by nonlinear state space description incorporating state and measurement equations

$$\vec{x}_{k+1}=f(\vec{x}_k,\vec{u}_k,{}^{w}{}_k) \quad (5)$$

$$\vec{z}_k=h(\vec{x}_k,\vec{v}_k) \quad (6)$$

In equation (5) nonlinear function (in general) relates the state vector $\vec{x}$ and the input $\vec{u}$ at time step *k* to the state at step *k+1*. In equation (6) measurement vector $\vec{h}$ relates the state vector to the measurement $\vec{z}_k$. Vectors $\vec{w}_k$ and $\vec{v}_k$ represent white process and measurement noise, respectively. It is assumed that these noises are Gaussian distributed, have zero mean and that they are uncorrelated.

During the EKF design process several filter architectures were tested. The chosen filter structure incorporates the state and measurement vectors defined as:

$$\vec{x}_k=\begin{bmatrix}\Theta_1\\ \dot{\Theta}_1\\ \ddot{\Theta}_1\\ \Theta_2\\ \dot{\Theta}_2\\ \ddot{\Theta}_2\\ \Theta_3\\ \dot{\Theta}_3\\ \ddot{\Theta}_3\end{bmatrix} \qquad \vec{z}_k=\begin{bmatrix}\dot{\Theta}_1\\ \dot{\Theta}_2\\ \dot{\Theta}_3\\ a_{y1}\\ a_{z1}\\ a_{y2}\\ a_{z2}\\ a_{y3}\\ a_{z3}\\ M_1\\ M_2\\ M_3\end{bmatrix}$$

where

$\Theta_1,\Theta_2,\Theta_3$ - shank, thigh and HAT angles in respect to *y* axis,

$\dot{\Theta}_1,\dot{\Theta}_2,\dot{\Theta}_3$ - shank, thigh and HAT angular rates of change,

$\ddot{\Theta}_1,\ddot{\Theta}_2,\ddot{\Theta}_3$ - shank, thigh and HAT angular accelerations

M_1,M_2,M_3 - ankle, knee and hip joint moments,

a_{yi} - linear acceleration of the *i*-th segment in *y* direction,

a_{zi} - linear acceleration of the *i*-th segment in *z* direction.

Variables in state and measurement vector are selected so that they can be measured directly or indirectly by inertial sensors. Directly measured variables are angular rates and linear accelerations (for every segment), while moments M_1,M_2 and M_3 are measured indirectly via inverse dynamic calculation using measured values.

The proposed EKF design has the advantage that the state equation

$$\begin{bmatrix} \dot{\Theta}_1 \\ \ddot{\Theta}_1 \\ \dddot{\Theta}_1 \\ \dot{\Theta}_2 \\ \ddot{\Theta}_2 \\ \dddot{\Theta}_2 \\ \dot{\Theta}_3 \\ \ddot{\Theta}_3 \\ \dddot{\Theta}_3 \end{bmatrix} = \begin{bmatrix} 0 & 1 & 0 & 0 & 0 & 0 & 0 & 0 & 0 \\ 0 & 0 & 1 & 0 & 0 & 0 & 0 & 0 & 0 \\ 0 & 0 & 0 & 0 & 0 & 0 & 0 & 0 & 0 \\ 0 & 0 & 0 & 0 & 1 & 0 & 0 & 0 & 0 \\ 0 & 0 & 0 & 0 & 0 & 1 & 0 & 0 & 0 \\ 0 & 0 & 0 & 0 & 0 & 0 & 0 & 0 & 0 \\ 0 & 0 & 0 & 0 & 0 & 0 & 0 & 1 & 0 \\ 0 & 0 & 0 & 0 & 0 & 0 & 0 & 0 & 1 \\ 0 & 0 & 0 & 0 & 0 & 0 & 0 & 0 & 0 \end{bmatrix} \cdot \begin{bmatrix} \Theta_1 \\ \dot{\Theta}_1 \\ \ddot{\Theta}_1 \\ \Theta_2 \\ \dot{\Theta}_2 \\ \ddot{\Theta}_2 \\ \Theta_3 \\ \dot{\Theta}_3 \\ \ddot{\Theta}_3 \end{bmatrix} \quad (7)$$

is linear, while measurement equation (8) is still highly non-linear.

$$\begin{bmatrix} h_1 \\ h_2 \\ h_3 \\ h_4 \\ h_5 \\ h_6 \\ h_7 \\ h_8 \\ h_9 \\ h_{10} \\ h_{11} \\ h_{12} \end{bmatrix} = \begin{bmatrix} \dot{\Theta}_1 \\ \dot{\Theta}_2 \\ \dot{\Theta}_3 \\ -c_1\ddot{\Theta}_1 \sin\Theta_1 - c_1\dot{\Theta}_1^2 \cos\Theta_1 \\ c_1\ddot{\Theta}_1 \cos\Theta_1 - c_1\dot{\Theta}_1^2 \sin\Theta_1 \\ -l_1\ddot{\Theta}_1 \sin\Theta_1 - l_1\dot{\Theta}_1^2 \cos\Theta_1 - c_2\ddot{\Theta}_2 \sin\Theta_2 - c_2\dot{\Theta}_2^2 \cos\Theta_2 \\ l_1\ddot{\Theta}_1 \cos\Theta_1 - l_1\dot{\Theta}_1^2 \sin\Theta_1 + c_2\ddot{\Theta}_2 \cos\Theta_2 - c_2\dot{\Theta}_2^2 \sin\Theta_2 \\ -l_1\ddot{\Theta}_1 \sin\Theta_1 - l_1\dot{\Theta}_1^2 \cos\Theta_1 - l_2\ddot{\Theta}_2 \sin\Theta_2 - l_2\dot{\Theta}_2^2 \cos\Theta_2 - c_3\ddot{\Theta}_3 \sin\Theta_3 - c_3\dot{\Theta}_3^2 \cos\Theta_3 \\ l_1\ddot{\Theta}_1 \cos\Theta_1 - l_1\dot{\Theta}_1^2 \sin\Theta_1 + l_2\ddot{\Theta}_2 \cos\Theta_2 - l_2\dot{\Theta}_2^2 \sin\Theta_2 + c_3\ddot{\Theta}_3 \cos\Theta_3 - c_3\dot{\Theta}_3^2 \sin\Theta_3 \\ M_2 + K_{11}\ddot{\Theta}_1 + K_{12}\ddot{\Theta}_2 \cos(\Theta_1 - \Theta_2) + K_{13}\ddot{\Theta}_3 \cos(\Theta_1 - \Theta_3) + K_{14}\dot{\Theta}_2^2 \sin(\Theta_1 - \Theta_2) + K_{15}\dot{\Theta}_3^2 \sin(\Theta_1 - \Theta_3) + K_{16} \cos\Theta_1 \\ M_3 + K_{22}\ddot{\Theta}_2 + K_{21}\ddot{\Theta}_1 \cos(\Theta_1 - \Theta_2) + K_{23}\ddot{\Theta}_3 \cos(\Theta_2 - \Theta_3) - K_{24}\dot{\Theta}_1^2 \sin(\Theta_1 - \Theta_2) + K_{25}\dot{\Theta}_3^2 \sin(\Theta_2 - \Theta_3) + K_{26} \cos\Theta_2 \\ K_{33}\ddot{\Theta}_3 + K_{31}\ddot{\Theta}_1 \cos(\Theta_1 - \Theta_3) + K_{32}\ddot{\Theta}_2 \cos(\Theta_2 - \Theta_3) - K_{34}\dot{\Theta}_1^2 \sin(\Theta_1 - \Theta_3) - K_{35}\dot{\Theta}_2^2 \sin(\Theta_2 - \Theta_3) + K_{36} \cos\Theta_3 \end{bmatrix} \quad (8)$$

In (8) meaning of the parameters is as follows

$$K_{11} = m_1 c_1^2 + m_2 l_1^2 + m_3 l_1^2 + I_{x1}$$
$$K_{12} = K_{14} = K_{21} = K_{24} = m_2 l_1 c_2 + m_3 l_1 l_2$$
$$K_{13} = K_{15} = m_3 l_1 c_3$$
$$K_{16} = g(m_1 c_1 + m_2 l_1 + m_3 l_1)$$
$$K_{22} = m_2 c_2^2 + m_3 l_2^2 + I_{x2}$$
$$K_{23} = K_{25} = K_{32} = K_{35} = m_3 l_2 c_3$$
$$K_{26} = g(m_2 c_2 + m_3 l_2)$$
$$K_{31} = K_{34} = m_3 l_1 c_3$$
$$K_{33} = m_3 c_3^2 + I_{x3}$$
$$K_{36} = m_3 g c_3$$

The EKF algorithm is implemented according to [9] as shown below

Measurement update is

$$\mathbf{K}_k = \mathbf{P}_k^- \mathbf{H}_k^T (\mathbf{H}_k \mathbf{P}_k^- \mathbf{H}_k^T + \mathbf{R}_k)^{-1} \quad (9)$$

$$\hat{\mathbf{x}}_k = \hat{\mathbf{x}}_k^- + \mathbf{K}(\mathbf{z}_k - \mathbf{h}(\hat{\mathbf{x}}_k^-, 0)) \quad (10)$$

$$\mathbf{P}_k = (\mathbf{I} - \mathbf{K}_k \mathbf{H}_k) \mathbf{P}_k^- \quad (11)$$

and time update is

$$\mathbf{P}_{k+1}^- = \mathbf{A}_k \mathbf{P}_k \mathbf{A}_k^T + \mathbf{Q}_k \quad (12)$$

$$\hat{\mathbf{x}}_{k+1}^- = \hat{\mathbf{x}}_k \quad (13)$$

Equations (9)-(13) form the complete set of equations for the EKF algorithm used in this paper. Matrix $\mathbf{P}$ defines estimate error covariance, while matrix $\mathbf{H}_k$ is the Jacobian matrix of partial derivates of $\mathbf{h}()$ with respect to $\mathbf{x}$:

$$\mathbf{H}_k = \frac{\partial h_i}{\partial x_j}(\mathbf{x}_k, 0) \quad (14)$$

The filter is in all instances initialized with a state estimate corresponding to the true system state.

3 Results

3.1 Results for simulated data

In order to validate the developed dynamic model and designed EKF, they were implemented in Matlab-Simulink environment and evaluated by simulated data.

The model (2), (3) and (4) was constructed in Simulink generating data for description of true model dynamics. The white noise with zero mean was added to data, simulating noisy sensor readings. In the simulation run the moments M_1, M_2 and M_3 were known in advance, and three-segment dynamic model was used in configuration of pendulum where the resulting motion was the result of joint moments M_1, M_2, M_3 and gravity. The inputs into EKF presented simulated sensor readings, while actual data was used for comparison. The sampling frequency in simulation run was 50Hz. The results of simulated three segment model motion and it's estimated joint angles are presented below.

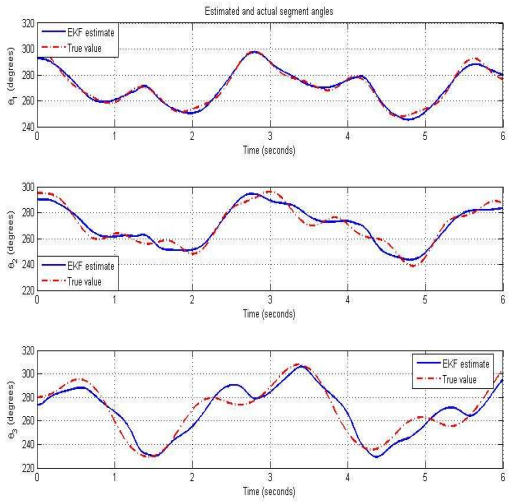

Fig. 2. Comparison of estimated and actual segment angels

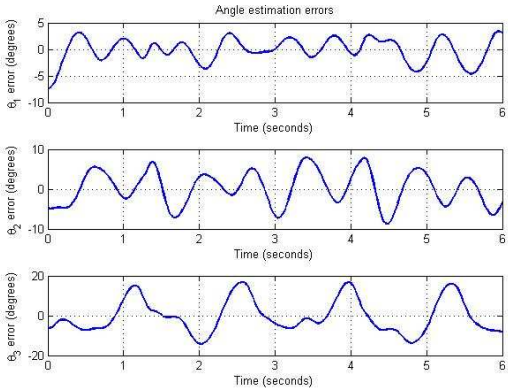

Fig. 3. Angle estimation errors

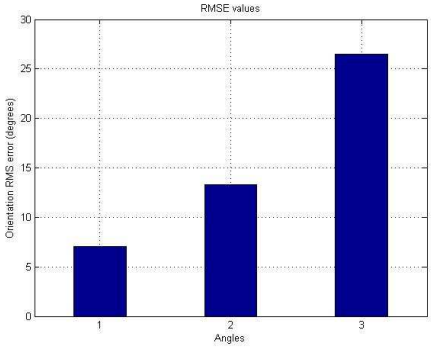

Fig. 4. Root mean square error (RMSE) for segment angle estimates

From presented results it can be seen that constructed dynamic human three-segment model and proposed EKF design perform well on simulated data. Smallest estimation errors occur for the first segment of the model while the error increases for subsequent segments. This is attributed to the fact that the equations for linear acceleration of second and especially third segment (h_6, h_7, h_8 and h_9 in equation (8)) are rather complex and depend on several system variables (e.g. equation for linear acceleration of third segment depends on angle of the first and second segment).

3.2 Results for measurement data

After validation by simulation, the same procedure was applied on real data measured with Optotrak optical motion capture system. Measurement setup can be seen in Figure 5. In measurement data certain amount of measurement noise is added, therefore higher discrepancies between estimated and Optotrak were expected.

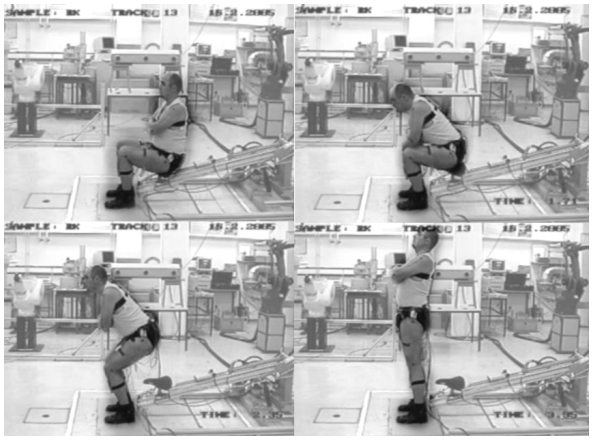

Fig. 5. Measurements with Optotrak optical motion analysis system

Moreover, the single and double differentiation is performed on measured data to obtain linear velocity and acceleration, respectively [2,9]. This procedure introduces additional error source (numerical error) to the signal.

Moments in ankle, knee and hip joint (M_1, M_2 and M_3) are not known in advance. They are calculated using Newton-Euler inverse dynamics approach before EKF implementation (see procedure on Fig. 6).

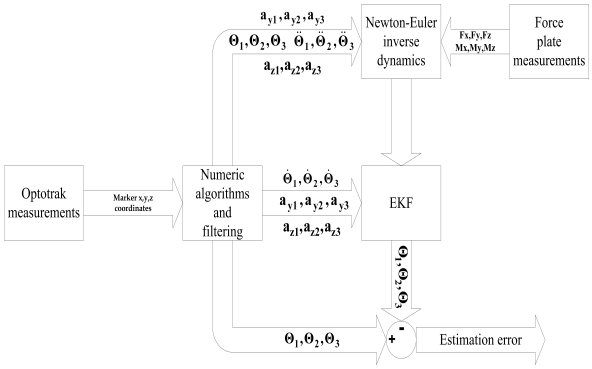

Fig. 6. Conceptual scheme of model based EKF implementation for human body kinematics reconstruction in standing up

As an example, calculated hip moment is presented in Fig. 7.

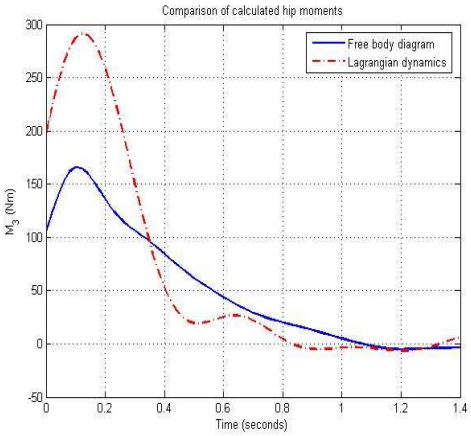

Fig. 7. Comparison of hip moment calculated with different methods

From Fig. 7 it can be seen that there is difference between hip moments calculated using Newton-Euler inverse dynamics/free body diagram approach (solid line) and using Lagrangian dynamics when measured angles, angular rates and angular accelerations are used in Equation (4). The difference is attributed to several reasons: a) simplifications are introduced to the model in modeling phase, b) the numerical errors are introduced during Optotrak data processing, c) in measurements no special care was taken to constrain subject with respect to sagittal plane. All of these facts contribute to difference in calculated hip moments. However the result makes possible to verify the performance of EKF filter in presence of large errors.

Comparison of estimation of three angles with angles obtained with Optotrak kinematic measurements are presented in Figure 8.

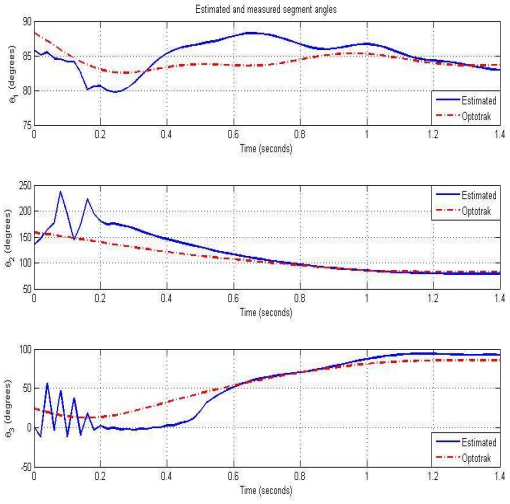

Fig. 8. Comparison of estimated segment angels with reference measurements obtained with Optotrak system

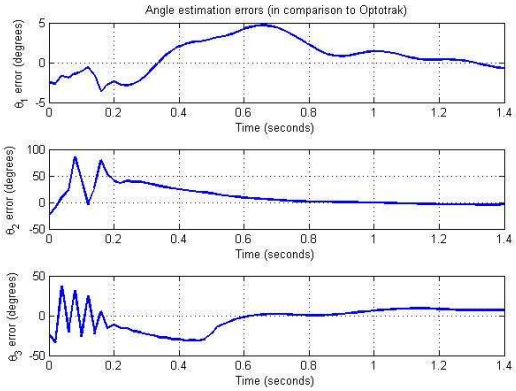

Fig. 9. Angle estimation errors in comparison to Optotrak measurements

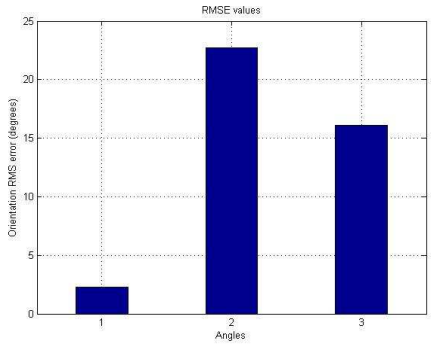

Fig. 10. Root mean square error (RMSE) for segment angle estimates in comparison to Optotrak measurements

From Figure 8 it can be seen that EKF takes some time to settle in (around 0.2 seconds), after which estimation error reduces and eventually becomes zero. Settling time of 0.2 sec is somewhat large for total time of 1.4 seconds, but we think this could be reduced by increasing measurement sampling rate. The tuning of EKF was done manually, what is time consuming and the procedure does not guarantee that the chosen matrices **R**, **Q** and **P** are optimal, so further improvements are needed and possible [13].

By inspecting estimation errors in Figure 9 similar conclusion can be drawn for all segments. Estimation error is large in the beginning while the EKF settles in, after that the error value decreases and approaches zero. Segment two (thigh) has the largest error in transition phase. This can be partially explained by large error in joint moment (M_2) measurement/calculation procedure.

Figure 10 depicts root mean square error values. As expected, the error is smallest for shank orientation estimation while it is largest for thigh orientation estimation. By comparing these values with those obtained from simulated runs, similar system performance in terms of RMSE can be observed. The only difference are larger measurement errors present in real measurements.

ISBN 978-3-901608-32-2

4 Conclusions

The procedure for reconstruction of motion trajectories of shank, thigh and HAT segment in sagittal plane during sit-to-stand movement using dynamic human body model and Extended Kalman filter is presented. The work is a first step toward development of measurement system based on miniature inertial sensors.

Good tracking performance is demonstrated on simulated motion of three-segment pendulum. The estimation error is the smallest for the shank orientation and it increases for every subsequent segment. This is primarily due to more complex (and coupled) equations used for segments 2 and 3 than for segment 1. It is worth noting that estimation error, although has large RMSE value for segments 2 and 3, oscillates around zero value meaning that the mean value is close to zero.

The tracking performance on measurement data is encouraging, however less accurate than in the case of simulated data. There are several reasons for this observation: a) low measurement sampling rate, b) numerical errors during signal processing, c) large errors in "measured" joint moments, d) manual EKF tuning, e) model simplifications and f) not ideal measurement setup. If all of these factors are taken into account we can conclude that the presented system performs well in presence of large errors.

To improve system performance in terms of estimation accuracy, certain improvements should be introduced. Higher sampling rate during measurement should improve EKF settling time. Introduction of automatic EKF tuning methods should also improve EKF estimation accuracy. More attention should be payed to measurement setup in regards to sagittal plane motion restriction. Significant improvements are expected by reducing the error in calculated joint moments. One direction could be to integrate joint moment calculation in EKF algorithm. Finally, three-segment dynamic human body model could be enhanced in a way that certain phenomenons (like joint friction) are included in the model.

The above improvements are planned to be incorporated in the system in the further development stage.

5 References

[1] R. Kamnik, J. Musić, H. Burger, M. Munih, T. Bajd. Design of Inertial Motion Sensors and its Usage in Biomechanical Analysis, *4th International Conference on Electrical and Power Engineering EPE 2006, 511-516,* Iasi, Romania, 2006

[2] A. Kralj, R. J. Jaeger, M. Munih. Analysis of standing up and sitting down in humans: definitions and normative data presentation, *Journal of Biomechanics*, 23(11): 1123-1138, 1990

[3] R. E. Mayagoitia, A. V. Nene, P. Veltink. Accelerometer and rate gyroscope measurement of kinematics: an inexpensive alternative to optical motion analysis system, *Journal of Biomechanics,* 35:537-542, 2002

[4] B. Najafi, K. Aminian, F. Loew, Y. Blanc, P. A. Robert. Measurement of Stand-Sit and Sit-Stand Transitions Using Miniature Gyroscopes and Its Application in Fall Risk Evaluation in the Elderly, *IEEE Trans. on Biomedical Engineering*, 49(8): 843-851, 2002

[5] M. C. Boonstra, . M. A. van der Slikke, N. L. W. Keijsers et al, The accuracy of measuring the kinematics of rising from chair with accelerometers and gyroscopes, *Journal of Biomechanics*,39(2): 354-358, 2006

[6] D. Roetenberg, P. J. Slycke, P. Veltink. Ambulatory Position and Orientation Tracking Fusing Magnetic and Inertial Sensing, *IEEE Trans. on Biomedical Engineering,* 54(4): 883-890, 2007

[7] X. Yun, E. R. Bachmann. Design, Implementation and Experimental Results of a Quaternion-Based Kalman Filter for Human Body Motion Tracking, *IEEE Trans. on Robotics*, 22(6): 1216-1227,2006

[8] C. Baten, P. Oosterhoff, I. Kingma, P. Veltink, H. Hermens. Inertial sensing in ambulatory back load estimation, *Proc. of 18th IEEE annual Int. conf*. 2(31): 497-498, 1996

[9] R. Kamnik, T. Bajd. Human Voluntary Activity Integration in the Control of a Standing-Up Rehabilitation Robot: A Simulation Study, *Medical engineering & physics*, 1-11, 2006

[10] D.Roetenberg, H. Luinge, P. Veltink. Inertial and magnetic sensing of human movement near ferromagnetic materials*, Proc. of 2nd IEEE and ACM International Symposium on Mixed and Augmented Reality*, 268-269, Tokyo, Japan, 2003

[11] H. Hemami, V. C. Jaswa. On a Three-Link Model of the Dynamics of Standing Up and Sitting Down, *IEEE Trans. on Systems, Man, and Cybernetics*, 8:115-120, 1978

[12] P.D. Leva. Adjustment to Zatsiorksy-Seluyanov's segment inertia parameters, *Journal of Biomechanics*, 29(9): 1223-1230, 1996

[13] P. Abbeel, A. Coates, M. Montemerlo, A. Ng, S. Thun. Discriminative Training of Kalman Filters, *Proc. of Robotics: Science and Systems '05*, Boston, 2005

